HAL
open science

Recent volcanic events and the distribution of hydrothermal venting at the Lucky Strike hydrothermal field, Mid-Atlantic Ridge

H. Ondréas, M. Cannat, Y. Fouquet, A. Normand, P. M Sarradin, J. Sarrazin

To cite this version:

H. Ondréas, M. Cannat, Y. Fouquet, A. Normand, P. M Sarradin, et al.. Recent volcanic events and the distribution of hydrothermal venting at the Lucky Strike hydrothermal field, Mid-Atlantic Ridge. Geochemistry, Geophysics, Geosystems, 2009, 10 (2), 10.1029/2008GC002171 . insu-01819621

HAL Id: insu-01819621

https://insu.hal.science/insu-01819621

Submitted on 20 Jun 2018

HAL is a multi-disciplinary open access archive for the deposit and dissemination of scientific research documents, whether they are published or not. The documents may come from teaching and research institutions in France or abroad, or from public or private research centers.

L'archive ouverte pluridisciplinaire **HAL**, est destinée au dépôt et à la diffusion de documents scientifiques de niveau recherche, publiés ou non, émanant des établissements d'enseignement et de recherche français ou étrangers, des laboratoires publics ou privés.

Geochemistry Geophysics Geosystems G3
AN ELECTRONIC JOURNAL OF THE EARTH SCIENCES
Published by AGU and the Geochemical Society

Article
Volume 10, Number 2
7 February 2009
Q02006, doi:10.1029/2008GC002171
ISSN: 1525-2027

Recent volcanic events and the distribution of hydrothermal venting at the Lucky Strike hydrothermal field, Mid-Atlantic Ridge

H. Ondréas
Géosciences Marines, Centre de Brest, IFREMER, BP 70, F-29280 Plouzané, France (helene.ondreas@ifremer.fr)

M. Cannat
Institut de Physique du Globe de Paris, CNRS, UMR 7154, 4 place Jussieu, Tour 14, F-75252 Paris CEDEX 05, France

Y. Fouquet and A. Normand
Géosciences Marines, Centre de Brest, IFREMER, BP 70, F-29280 Plouzané, France

P. M. Sarradin and J. Sarrazin
Environnement Profond, Centre de Brest, IFREMER, BP 70, F-29280 Plouzané, France

[1] We present new high-resolution bathymetry and backscatter data acquired in 2006 with the ROV *Victor 6000* over the Lucky Strike hydrothermal field, Mid-Atlantic Ridge. As long-term monitoring of the Lucky Strike area (MoMAR project) is being implemented, these new high-resolution data offer an unprecedented view of the distribution of hydrothermal edifices, eruptive facies, and small-scale tectonic features in the Lucky Strike vent field. We show that vents located in the NW and NE correspond with wide expanses of lumpy seafloor which we interpret as primarily made of broken chimneys and sulfide edifices. They are found above scarps with relief >50 m or on associated mass wasting deposits. By contrast, the SE and SW vents correspond with small expanses of lumpy seafloor and are located near smaller scarps which we interpret as more recent faults. Hydrothermal edifices in the SW venting area appear very recent, postdating the emplacement and faulting of the most recent lava. We propose that this difference in the age of hydrothermal edifices does not mean that hydrothermal venting itself is more recent in the southern part of the Lucky Strike field because preexisting sulfide deposits there may have been buried by recent volcanic deposits. Instead, the older edifices in the northern part of the hydrothermal field may have been allowed more time to grow because they are set above the level of recent lava flows. The formation of a lava lake is the most recent eruptive event detected at Lucky Strike. Lava drainback is evidenced by benches and lava pillars, suggesting a close connection with an underlying magma reservoir, which probably corresponds to the melt body imaged by Singh et al. (2006). We have found no evidence that this lake was active for months to decades, as lava lakes at terrestrial volcanoes. It may instead have formed as a lava pond, with successive lava flows covering the eruptive vents, as proposed for similar features at the EPR. The horizontal surface of the lake is deformed only near its southwestern shore, along a NNE-trending set of faults and fissures, which appear to control the distribution of hydrothermal chimneys.

Components: 10,391 words, 7 figures, 1 table.

Keywords: Mid-Atlantic Ridge; Lucky Strike; lava lake; hydrothermalism.

Copyright 2009 by the American Geophysical Union

Index Terms: 3017 Marine Geology and Geophysics: Hydrothermal systems (0450, 1034, 3616, 4832, 8135, 8424); 8416 Volcanology: Mid-oceanic ridge processes (1032, 3614); 8414 Volcanology: Eruption mechanisms and flow emplacement.

Received 15 July 2008; **Revised** 15 September 2008; **Accepted** 22 October 2008; **Published** 7 February 2009.

Ondréas, H., M. Cannat, Y. Fouquet, A. Normand, P. M. Sarradin, and J. Sarrazin (2009), Recent volcanic events and the distribution of hydrothermal venting at the Lucky Strike hydrothermal field, Mid-Atlantic Ridge, *Geochem. Geophys. Geosyst.*, *10*, Q02006, doi:10.1029/2008GC002171.

1. Introduction

[2] High-resolution mapping of the seafloor started at fast spreading ridges during the last decade, with the help of submersible-borne scanning sonars [*Kurras et al.*, 1998; *Chadwick et al.*, 2001; *Cormier et al.*, 2003; *Tanaka et al.*, 2007]. These studies allow resolutions of the order of a few decimeters, over areas of a few thousand square meters. This scale is intermediate between that of shipboard multibeam surveys and the finer scale of submersible geological observations and sampling. Such high-resolution maps are therefore critical tools to link regional structures and local geology and to prepare sampling strategies or long-term monitoring.

[3] High-resolution mapping studies of slow spreading systems are still few. *Edwards et al.* [2001] conducted a side scan survey of the Gakkel Ridge. *Humphris and Kleinrock* [1996] analyzed the morphology of the TAG hydrothermal mound based on near bottom high-resolution bathymetry. *Scheirer et al.* [2000] and *Humphris et al.* [2002] completed a DSL-120 sonar survey of the Lucky Strike area with a resolution of 1–2 m for the side scan and 4 m for the bathymetry. The data we report in this paper, with nominal resolutions of 0.4 m and 1.5 m for the bathymetry, are the first very high-resolution data for the slow-spreading Mid-Atlantic Ridge (MAR). They were acquired in 2006 during the MoMAReto cruise of N.O. *Pourquoi Pas?*, with a SeaBat 7125 multibeam echo sounder installed on the *Victor* ROV. With long-term multidisciplinary monitoring of the Lucky Strike hydrothermal area just beginning, these data offer an unprecedented view of the distribution of eruptive facies, small-scale tectonic and mass-wasting features, and hydrothermal vents in the Lucky Strike vent field. These data can also be used as a baseline to detect future topographic changes in the area. In this paper, we use these high-resolution data to specifically address two issues: the geological context and the extent of active and recent hydrothermal venting at Lucky Strike, and the recent eruptive and tectonic history of the summit area of the Lucky Strike volcano. We use dive and sampling observations from previous cruises as ground truth for our interpretations.

2. Regional Setting of the Lucky Strike Segment

[4] The Lucky Strike segment, located between 37°03′N and 37°37′N, 400 km southwest of the Azores Islands, is 60 km long (Figures 1a and 1b). Spreading in this region of the MAR occurs with a N110° direction, at a rate of 22 mm/a according to both the NUVEL1 model [*DeMets et al.*, 1990], and the local pattern of magnetic anomalies [*Cannat et al.*, 1999]. Lucky Strike lies on the long wavelength gradient of decreasing axial depths and gravity anomalies which characterizes the present-day influence of the Azores hot spot on the MAR [*Detrick et al.*, 1995]. The ridge segment to the north of Lucky Strike (the Menez Gwen segment) marks the southern edge of the Azores platform. It has an average axial depth around 2000 m and a mean crustal thickness that is about 1 km thicker than normal oceanic crust values [*Detrick et al.*, 1995; *Escartin et al.*, 2001]. The Lucky Strike segment shallows at its center due to a large central volcano (Figure 1), but the ends of the segment have the same depth (about 3000 m) as the MAR segments to the south. Its average crustal thickness, as inferred from gravity [*Detrick et al.*, 1995; *Escartin et al.*, 2001], is 6.3 km, near normal oceanic crust values [*Chen*, 1992]. Most basalts from Lucky Strike are, however, enriched in incompatible elements relative to normal MORB [*Langmuir et al.*, 1997; *Dosso et al.*, 1999; *Ferreira et al.*, 2005]. This shows that, while not producing very large excess melt, the mantle beneath the Lucky Strike segment includes a hot spot-derived component. This enrichment of the magmatic rocks is reflected in the composition of the fluids that vent in the Lucky Strike hydrothermal field [*Langmuir et al.*, 1997].

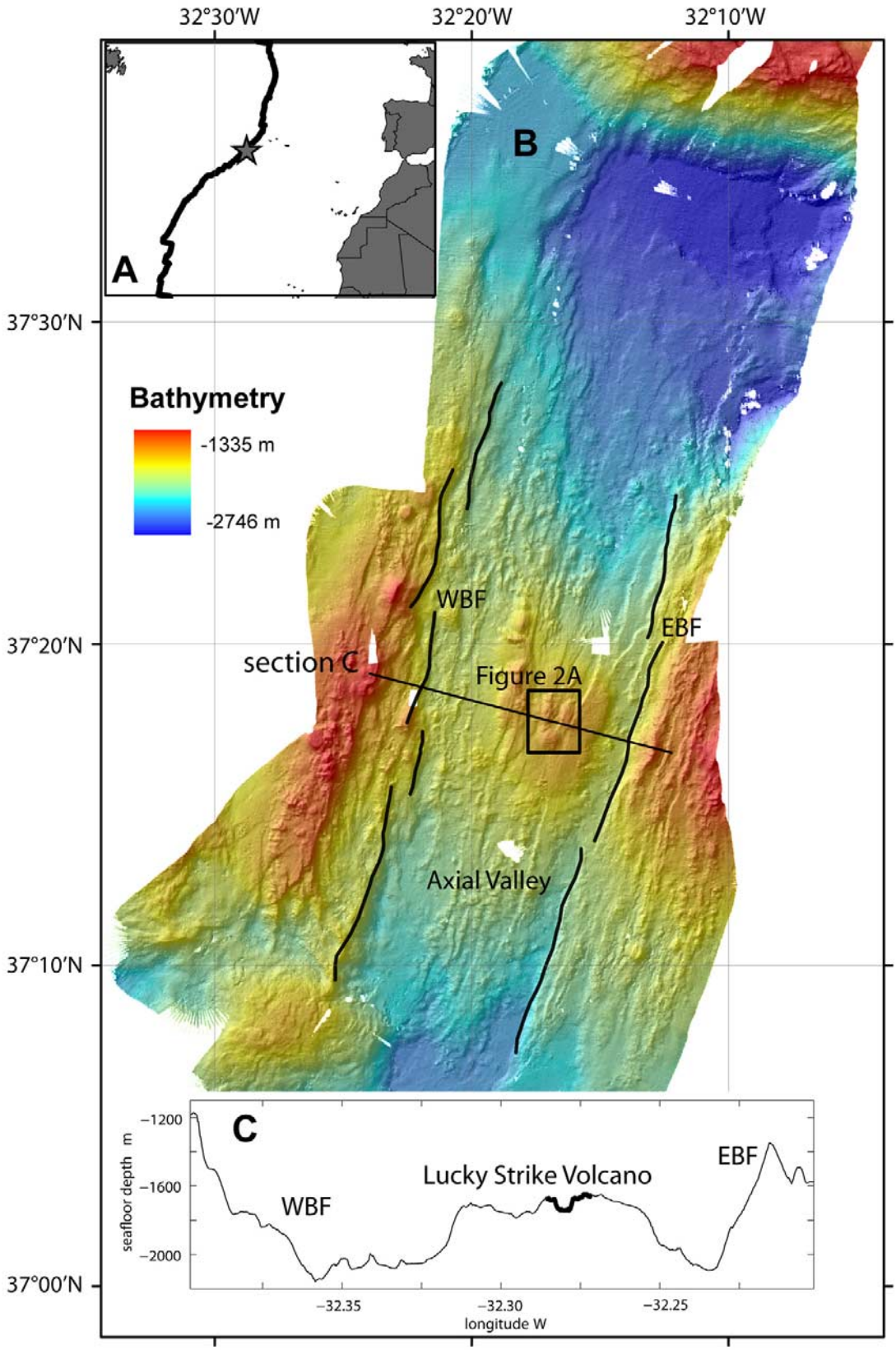
32°30′W
32°20′W
32°10′W
37°30′N
37°20′N
37°10′N
37°00′N
A
B
Bathymetry
-1335 m
-2746 m
WBF
EBF
section C
Figure 2A
Axial Valley
C
seafloor depth m
−1200
−1600
−2000
WBF
Lucky Strike Volcano
EBF
−32.35
−32.30
−32.25
longitude W

Figure 1

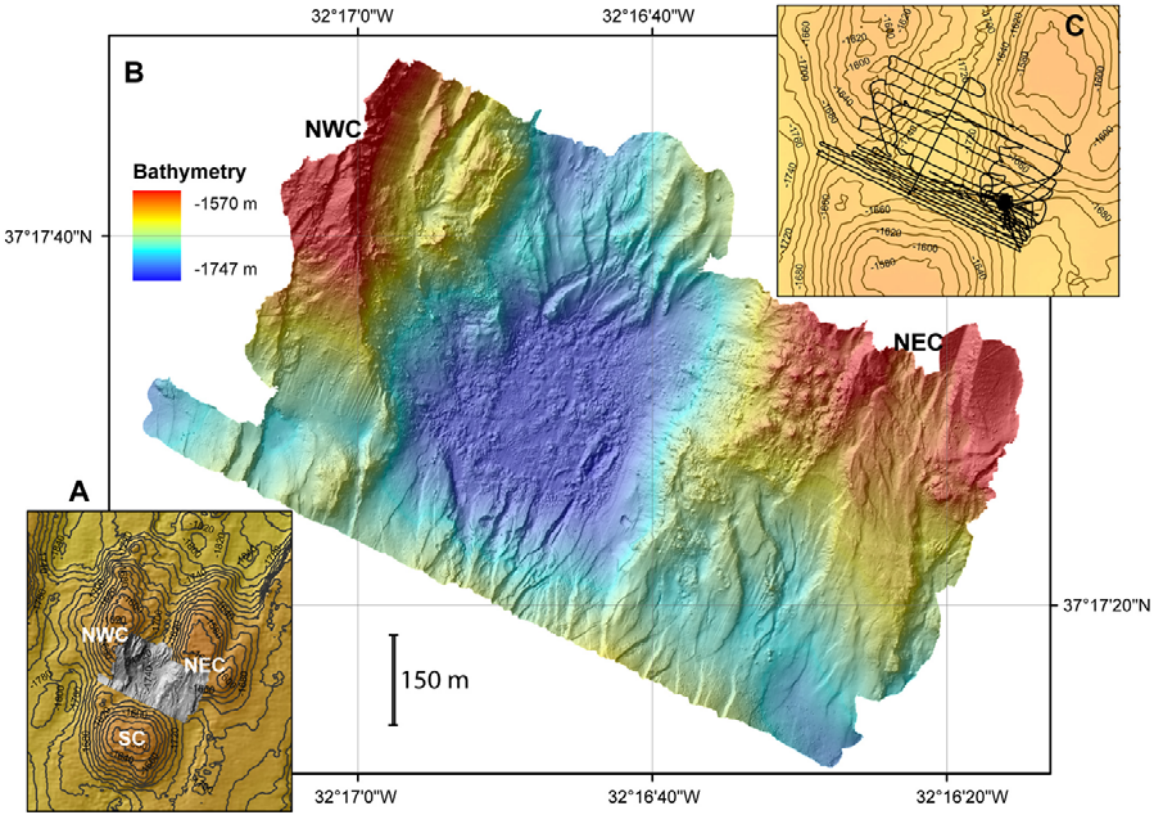

Figure 2. (a) Map and (b) shaded high-resolution MMR bathymetry of the Lucky Strike hydrothermal field. (c) Tracks of the ROV *Victor* during the MMR survey. NWC: Northwest volcanic Cone; NEC: Northeast volcanic Cone; SC: South volcanic Cone.

[5] The Lucky Strike segment exhibits a 10–15 km wide axial valley floor, bounded by inward facing, 1000-m high, axial valley walls (Figure 1c). The volcano at the center is 13 km along-axis, about 7 km across-axis, and more than 400 m high. At some time after its formation, it has been rifted in two parts separated by a 3 to 5 km wide, NNE-trending, and 50 to 100 m-deep graben. The three volcanic cones that form the present-day summit of the volcano are located near the eastern wall of this graben. These three cones surround a 1-km-diameter, 100-m deep depression, which hosts most of the venting sites [*Ondréas et al.*, 1997, *Humphris et al.*, 2002]. The fossil lava lake is set in the center of this depression. It is 300 m in diameter [*Fouquet et al.*, 1995b] and made of fresh lobate and sheet flows, small pillow mounds (2 m high), and collapsed lobate lava. It shows very little fissuring and has therefore been interpreted as a product of the most recent eruptions [*Humphris et al.*, 2002].

3. Lucky Strike Hydrothermal Field

[6] The Lucky Strike hydrothermal field was discovered during the FAZAR French-American cruise in 1992 [*Langmuir et al.*, 1993; *Wilson et al.*, 1996]. A rock dredge between the three summit cones of the axial volcano at the center of the Lucky Strike segment (Figure 1 and Figure 2a) recovered part of a sulfide chimney with live mussels. The vent field was first investigated in situ by *Alvin* in June 1993 [*Langmuir et al.*, 1993, 1997] and several active vents were found. Since then, the Lucky Strike area has been studied by

Figure 1. (a) Bathymetric map of the Lucky Strike segment from shipboard multibeam data acquired at low speed during the FLORES cruise of R/V *L'Atalante*. Lines show the location of the main axial valley bounding faults (WBF: west bounding faults; EBF: east bounding faults). Black square shows the location of Figure 2a, over the summit of the central volcano. (c) The across-axis shape of this volcano (summit area, corresponding to the high-resolution "Module de Mesures en Route" (MMR) survey of Figure 2, is shown bold). Vertical exaggeration is 5.5 times.

numerous international submersible or ROV cruises. European teams returned to the area for Nautile dives during the DIVA 1 cruise in 1994 and for the HEAT program during which the TOBI deep-tow side scan sonar system was used [*Parson et al.*, 2000]. Then the LUSTRE program [*Fornari et al.*, 1996; *Humphris et al.*, 1996] conducted another deep-tow side scan sonar survey with the DSL-120 system, Argo II optical and acoustic imaging, and dives of the ROV *Jason* [*Scheirer et al.*, 2000; *Humphris et al.*, 2002]. Thirty Nautile dives were carried out during the FLORES cruise in 1994 [*Fouquet et al.*, 1995a], and in 2001, the IRIS cruise completed a comprehensive ROV *Victor* survey of Lucky Strike vents. Finally during the summer 2006, both the ROV *Victor* and the Nautile submersible were on site during the MoMAReto (R/V *Pourquoi Pas?*) [*Sarrazin et al.*, 2006] and GRAVILUCK (R/V *l'Atalante*) cruises, for the initial implementation of long-term monitoring of the Lucky Strike area as part of the MoMAR (Monitoring the Mid-Atlantic Ridge) project.

[7] The Lucky Strike hydrothermal vent field extends over 1 km^2 on the summit of a prominent volcano, at the center of the Lucky Strike segment of the Mid-Atlantic Ridge (Figure 1). Venting sites at Lucky Strike comprise flanges with pool temperatures higher than 200°C, and black smokers, venting fluids as hot as 333°C [*Charlou et al.*, 2000] and chimneys discharging lower temperature diffuse fluids. Hydrothermal venting occurs in four main areas, each comprising a number of chimneys (Table 1): the northeastern area (Sintra, Statue of Liberty), the northwestern area (Jason, Bairro Alto, Elisabeth), the southwestern area (Helene, Nuno, Crystal, White Castel, Pico), and the southeastern area (Isabel, Tour Eiffel, markers U.S. 4, 6, 7, Chimiste, Montsegur). Studies of fluid temperature and chemistry suggest that the northern and western vents are fed by a hydrothermal source that is distinct from that feeding the southeastern vent sites [*Langmuir et al.*, 1997; *Von Damm et al.*, 1998, *Charlou et al.* 2000]. In addition, *Charlou et al.* [2000] proposed that the highest silica concentration of 16 mmol/kg found at Lucky Strike indicates that the main water-rock reaction zone occurs at depths >1.3 km.

[8] The vents at Lucky Strike surround a flat expanse of ropy lava and spectacular pillar structures, interpreted as a fossil lava lake [*Fouquet et al.*, 1995b]. The discovery of this lava lake suggested that a crustal magma chamber exists, or was recently active, beneath the Lucky Strike volcano [*Fouquet et al.*, 1995b]. This has been confirmed recently with the discovery of an axial magma chamber (AMC) reflector, similar to those observed at faster spreading ridges, and interpreted as the roof of a crustal melt lens [*Singh et al.*, 2006]. This inferred melt lens lies at a depth of 3 to 4 km beneath seafloor (bsf). It extends 1 to 3 km across axis [*Combier et al.*, 2007] and 7 km along-axis [*Singh et al.*, 2006]. It is underlain by a low-velocity lower crustal domain, interpreted as hot gabbroic rocks with a small proportion of melt [*Seher et al.*, 2007].

[9] Hydrothermal vents to the south and the west of the lava lake are built upon a distinctive formation of layered basaltic breccia, sometime silica-cemented, that forms a slab-like material up to a meter thick [*Langmuir et al.*, 1997; *Ondréas et al.*, 1997; *Humphris et al.*, 2002]. This slab formation has been interpreted as hyaloclastite deposit, formed during local explosive volcanic activity [*Fouquet et al.*, 1998; *Eissen et al.*, 2003] and later cemented by silica precipitated from mixtures of hydrothermal fluids and seawater [*Humphris et al.*, 2002]. The three volcanic cones, and most lesser topographic highs in the summit area, are made of pillow basalts, with highly vesicular plagioclase-phyric lava and basaltic breccia [*Ondréas et al.*, 1997; *Humphris et al.*, 2002]. Layered volcaniclastic deposits similar to the inferred protolith of the slab formation are also present within the central depression [*Ondréas et al.*, 1997; *Fouquet et al.*, 1998; *Eissen et al.*, 2003].

[10] The fault and fissure pattern in the summit area of the Lucky Strike volcano has been analyzed by *Parson et al.* [2000] based on TOBI side scan sonar data, and by *Scheirer et al.* [2000] and *Humphris et al.* [2002], based on DSL-120 side scan sonar data and on seafloor imagery. *Scheirer et al.* [2000] have described the three summit cones as made of series of subparallel, N10-N30 trending ridges and troughs, with a relief of 10 to 20 m. These authors show a neo-volcanic zone that is ~1 km wide and extends to the NNE and SSW from the area of the lava lake. This definition of the neovolcanic axis appears to fit with magnetic anomalies modeled from shipboard surveys [*Miranda et al.*, 2005].

4. Data and Methods

[11] The high-resolution bathymetry and backscatter data (Figures 2 and 3) analyzed in this paper were acquired during the MoMAReto cruise of R/V *Pourquoi Pas?*. A new survey module called

Table 1. Coordinates of Hydrothermal Sites in the Lucky Strike Vent Field[a]

Site Name	Latitude (Exomar)	Longitude (Exomar)	Shifted Latitude	Shifted Longitude	Reported Depth (m)	Reference for Reported Depth	Depth on High-Resolution Map (m)	Markers
Helene	N 37 17.4900	W 032 16.8800			1722	C2000	1716	Flores 17
Pico	N 37 17.4400	W 032 16.8900					1736	Pico
Bairro Alto	N 37 17.6300	W 032 16.9600					1662	Flores 21, PP7, PP8
Chimiste	N 37 17.3700	W 032 16.5900			1648	C2000	1685	
Tour Eiffel	N 37 17.3440	W 032 16.5330			1687	LR + VD98	1690	Flores 16, Diva II, IV, V, VI
Sintra	N 37 17.5100	W 032 16.4700			1618	LR + VD98	1632	Flores 15, US3
St. Liberty	N 37 17.5600	W 032 16.5700	N 37 17.5566	W 032 16.4729	1630	LR + VD98	1622	US1
Isabel	N 37 17.3700	W 032 16.6400	N 37 17.3935	W 032 16.6344	1685	C2000	1682	Flores 22, Diva VIII
Elisabeth	N 37 17.6300	W 032 16.8700					1696	PP12, PP13
US7	N 37 17.2870	W 032 16.5660			1708	VD98	1701	US7
Y3	N 37 17.5047	W 032 16.6704			1729	C2000	1730	Flores 14, Diva I
Montsegur	N 37 17.2760	W 032 16.5380			1700	C2000	1704	
US4	N 37 17.2760	W 032 16.5380			1700	LR + VD98 + C2000	1704	US4
Nuno	N 37 17.4900	W 032 16.9300	N 37 17.4835	W 032 16.9035	1727	C2000	1738	Flores 19, Diva X
US6	N 37 17.2990	W 032 16.5660			1703	LR + VD98 + C2000	1703	US6
PP4	N 37 17.4300	W 032 16.5900			1665		1676	PP4
	Latitude (Lustre)	Longitude (Lustre)						
2608 Vent	N 37 17.5100	W 032 16.6600			1719	LR + VD98	1725	
Jason	N 37 17.6500	W 032 16.9000			1644	LR + VD98	1662	
Crystal	N 37 17.4500	W 032 16.9200			1726	LR + VD98	1722	
White Castle	N 37 17.4400	W 032 16.9300			1724	LR	1720	

[a] Coordinates proposed after the EXOMAR and LUSTRE cruises are listed in the first two columns. Shifted coordinates are proposed for three sites on the basis of the new high-resolution map (see text). Depth reported for each site is listed with the corresponding references (C2000 for *Charlou et al.* [2000]; VD98 for *Von Damm et al.* [1998]; LR for the LUSTRE Cruise Report). The last column lists the names of markers which have been deployed at each site.

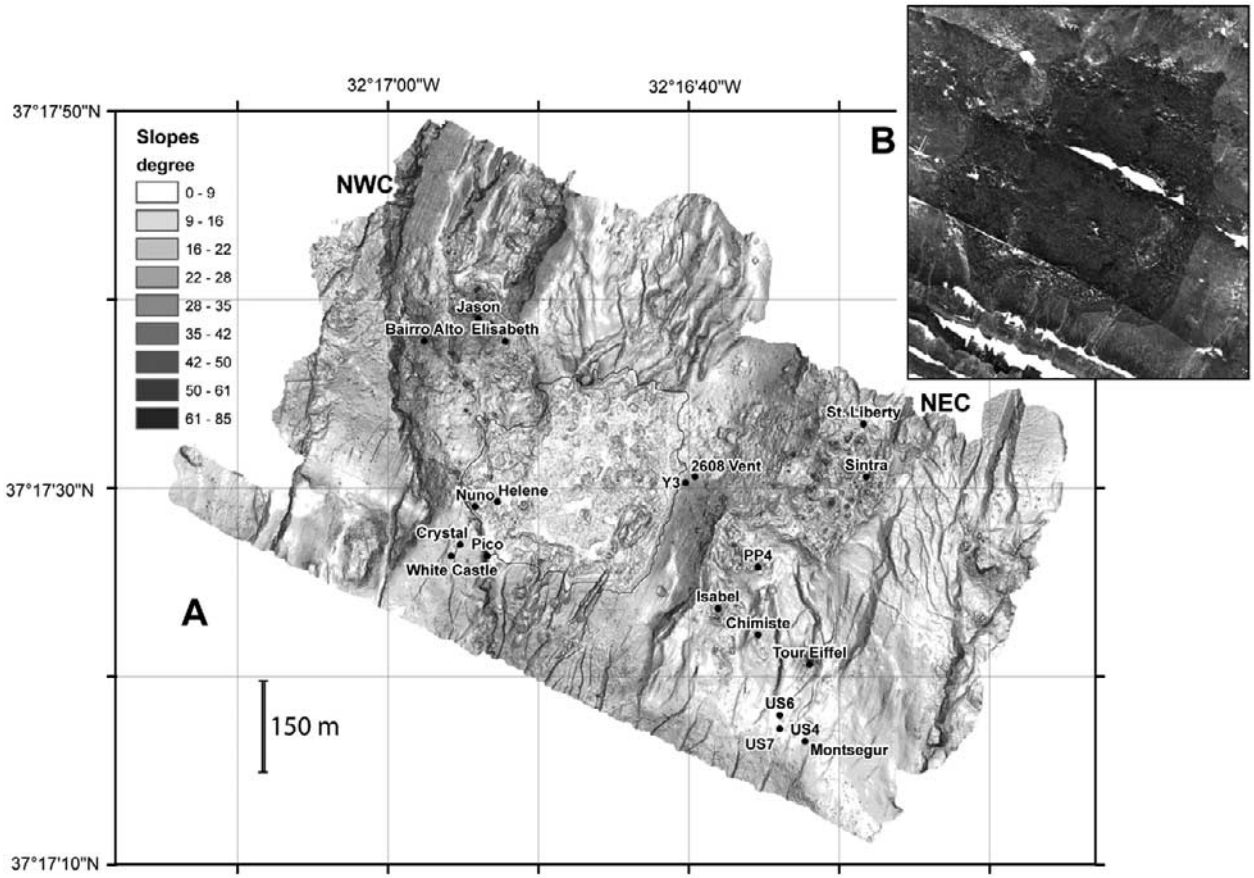

Figure 3. (a) Slope map calculated for the high-resolution MMR bathymetry of the Lucky Strike hydrothermal field. Coordinates for most known hydrothermal sites are extracted from submersible navigation recorded during the LUSTRE, DIVA, and EXOMAR cruises. Coordinates for the White Castle, Crystal, Jason, and 2608 vents from *Scheirer et al.* [2000] and *Humphris et al.* [2002]. The thin black line is the limit of the lava lake as drawn from (b) high-resolution MMR reverse backscatter data. NWC: Northwest Volcanic Cone; NEC: Northeast Volcanic Cone.

"Module de Mesures en Route" (MMR) was deployed on ROV *Victor 6000* during this cruise. This module acquires real time chemical, acoustic, and visual data [*Sarrazin et al.*, 2006; *Siméoni et al.*, 2007]. It includes a RESON SeaBat 7125 multibeam echo sounder for high-resolution mapping. This system operates with a frequency of 400 kHz, to a maximum altitude (H) of 200 m above seafloor. At an altitude of 100 m, it offers up to 120° swath coverage. It has a horizontal resolution of 5% of H, and a bathymetric accuracy of 0.2% of H. The ROV *Victor* is navigated with an ultrashort baseline system. Accuracy is about 1% of seafloor depth. The ROV also uses a dead-reckoning navigation system. During the survey, the ROV came back every 2 h to a marker and this dead reckoning system was reset. This allowed us to estimate a maximum drift of about 10 m per 2 h.

[12] The MoMAReto MMR survey area (Figures 2a and 2b) extends over 1200 m by 800 m between the three volcanic cones at the summit of the Lucky Strike central volcano. Data were collected along 15 profiles oriented N110, 8 profiles were spaced by 20 m and navigated at an altitude of 8 m, and the remaining 7 profiles were spaced by 70 m and navigated at an altitude of 30 m (Figure 2c). Two perpendicular cross-lines were also acquired. The nominal horizontal resolution was therefore 0.4 m for the first 8 profiles and 1.5 m for the remaining 7 profiles. Both sets of data were gridded together at a grid point spacing of 0.5 m (this grid is available at 1m spacing in the auxiliary material).[1]

[13] Seafloor reflectivity data (backscatter) were also collected along the same tracks (Figure 2c and Figure 3b). High-resolution ROV bathymetry and reflectivity data were processed with the CARAIBES® software (Ifremer). We also used

[1]Auxiliary materials are available in the HTML. doi:10.1029/2008GC002171.

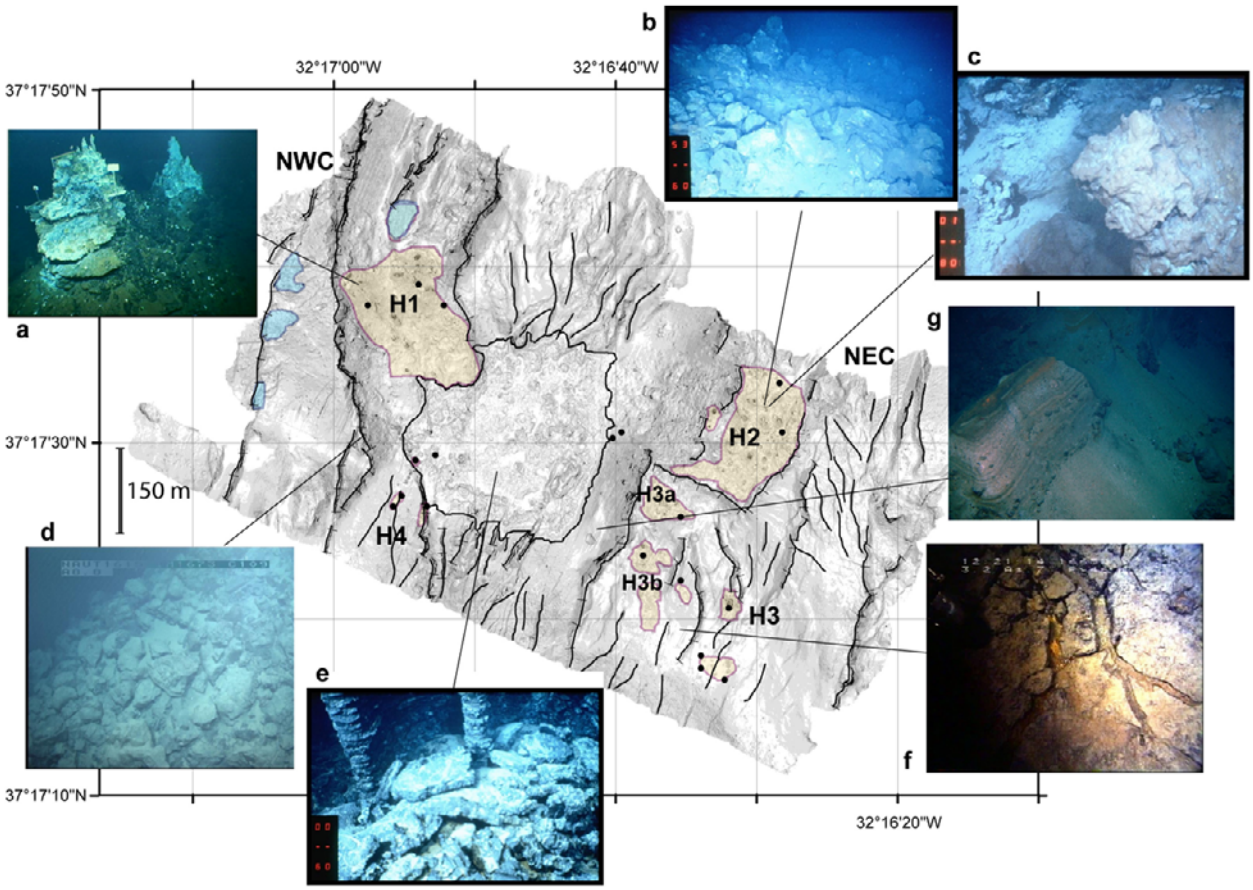

Figure 4. Sketch map of the Lucky Strike hydrothermal field, with slope map (as in Figure 3) in background. Yellows domains correspond to areas with abundant inferred hydrothermal edifices and sulfide debris, where active and dead chimneys have been observed. They correspond to the "lumpy morphology" referred to in the text. Blue domains correspond to domains where hydrothermal activity is inferred based on scarce dive data. Black contour is the limit of the lava lake as in Figure 3. Black lines outline the principal scarps. H1, H2, H3, and H4 are hydrothermal areas discussed in text. NWC: Northwest Volcanic Cone; NEC: Northeast Volcanic Cone. Dive photographs illustrate the main rock facies referred to in text as follows: (a) active hydrothermal chimneys; (b) sulfide debris; (c) dead chimney; (d) talus of pillow basalt; (e) lava pillars; (f) fissures in the slab formation; (g) layered volcaniclastic deposit. Each picture represents about 5 by 5 m.

high-quality shipboard multibeam data obtained at slow speed and narrow beam during the FLORES cruise (Figure 1b). We used the GIS-based ADELIE software (Ifremer Data Processing Department) to relocate in situ observations and sampling locations from six Nautile and ROV *Victor* cruises: the DIVA cruise in 1994; FLORES in 1997; IRIS in 2001; EXOMAR in 2005, MoMAReto and GRAVILUCK in 2006.

5. Results

[14] The MoMAReto high-resolution survey covers the central fossil lava lake, as well as all known vent sites at Lucky Strike (Figure 2 and Figure 3). It resolves features such as the largest hydrothermal edifices and allows us to draw the contours of the fossil lava lake with a much higher precision than provided in previous publications (Figures 3a and 3b). We first analyze the morphology of the seafloor at and near known active and inactive vent sites. We then describe our observations in the fossil lava lake and in the surrounding fissured terrains.

5.1. Geological Context of Hydrothermal Venting at Lucky Strike

[15] The resolution of the new survey is such that the highest hydrothermal edifices can be singled out as spiky highs, while the surrounding seafloor, with smaller edifices, broken chimneys, and flanges, is characterized by a lumpy morphology (lumps typically are 20 to 30 m in diameter and 5 to 10 m in height; Figures 3 and 4). We have

compiled the locations proposed for Lucky Strike vent sites in the work of *Charlou et al.* [2000], *Scheirer et al.* [2000], *Humphris et al.* [2002], and in the EXOMAR cruise report (Table 1). Because the original navigation of dives which have explored these sites so far had relatively large uncertainties, plotting of these locations on the high-resolution map resulted in locally significant misfits. The high-resolution bathymetry helped resolve some of these misfits (Figures 3 and 4): for example, previously proposed locations for the Isabel chimney plotted up to 40 m away from a prominent and isolated spike in the bathymetry. For some other known vents it was, however, difficult to decide to which spike on the map they correspond. The coordinates proposed by *Charlou et al.* [2000] for the Nuno and Helene vents are clearly wrong because they plot off the map. The EXOMAR cruise report located these two sites in the lava lake. On the basis of dive observations, we have moved the Nuno site by 40 m to the western lava lake shore. For the other vent sites, we have kept the coordinates proposed in the most recent publications and compiled in the EXOMAR cruise report. These coordinates are listed in Table 1 and plotted in Figure 3. There are also ambiguities in some instances on whether nearby vents identified as distinct in the literature are indeed distinct, or the same vents which would have been named twice. This may be the case for example for site Y3, a 3–4 m high smoker near the eastern shore of the lava lake, which probably corresponds to the 2608 site. We also do not know the exact correspondence between the Crytal/White Castle and Nuno/Helene sites. We anticipate that future dives in the area will clarify these ambiguities.

[16] The resolution of the new data also allows us to single out the bathymetric signature of large sulfide edifices: a lumpy morphology with circular spiky highs (Figures 3a and 4). This signature characterizes large known vent sites, but is also found in other areas where it is inferred to correspond to active or fossil edifices which are not listed in Table 1. On the basis of previous seafloor observations and new high-resolution imagery, four areas of venting are identified. The two northern venting areas (H1 and H2 in Figure 4) are the most extensive, with a number of large, probably fossil edifices and talus of massive sulfides which surround the known active vents [*Ondréas et al.*, 1997; *Humphris et al.*, 2002]. This is particularly the case for the northeastern area (H2 in Figure 4). By contrast, the seafloor morphology characteristic of sulfide edifices appears restricted to the vicinity of known active sites in venting area H3, while there are no resolvable lumpy morphological domains associated with the southwestern vents (venting area H4), or with the isolated Y3–2068 vent(s) near the fossil lava lake (Figure 3a and Figure 4). This suggests that hydrothermal venting there is more recent or more diffuse. In the following paragraphs we detail the setting and main characteristics of each venting area.

5.1.1. NW Hydrothermal Venting Area

[17] The NW hydrothermal venting area (H1 and a in Figure 4) includes known active vents such as Bairro Alto, Elisabeth, and Jason (Figure 3a). It extends some 200 m by 150 m over the steep east-facing slope that bounds the Northwestern Volcanic Cone. The upper edge of this slope corresponds to a somewhat curvilinear NNW to SSE-trending scarp (Figures 2 to 4). This scarp explored during dives cuts into formations of pillows and brecciated pillows (Figure 4d). The middle and lower slopes are formed by mass-wasting, with hydrothermal venting set on the resulting talus which is locally dominated by debris of massive sulfide. The total maximum heave (scarp plus talus-covered slope) for this Northwestern Volcanic Cone scarp is 130 m (Figure 5; sections 4 to 7). Although this heave may have originated as a tectonic vertical displacement, the curvilinear shape of the scarp suggests that it is now the scar of a large slump which extends to the north another kilometer or so, outside of our mapped area and forms the eastern flank of the Northwest Volcanic Cone (Figure 2a). To the north of the NW hydrothermal venting area, this slope comprises two secondary scarps, the upper one is up to 16 m high, and the lower one is up to 50 m high (Figure 5; sections 1 to 3). These two secondary scarps may also be primarily controlled by gravity sliding.

[18] Lumpy seafloor morphologies similar to those associated with known hydrothermal vents in the NW venting area, are also found over a small area to the north of the Jason vent (Figure 4, areas in blue), and along the NNE-trending, rectilinear scarp (heave about 12–15 m; Figure 5 sections 3 to 9) to the west of the main Northwest Volcanic Cone scarp (also outlined in blue in Figure 4). Although no vents have yet been discovered there, white and yellow patches that are characteristic of hydrothermal flanges have been observed from a distance in the southern part of this area during dives devoted to geodesic studies (GRAVILUCK cruise; V. Ballu personal communication, 2006).

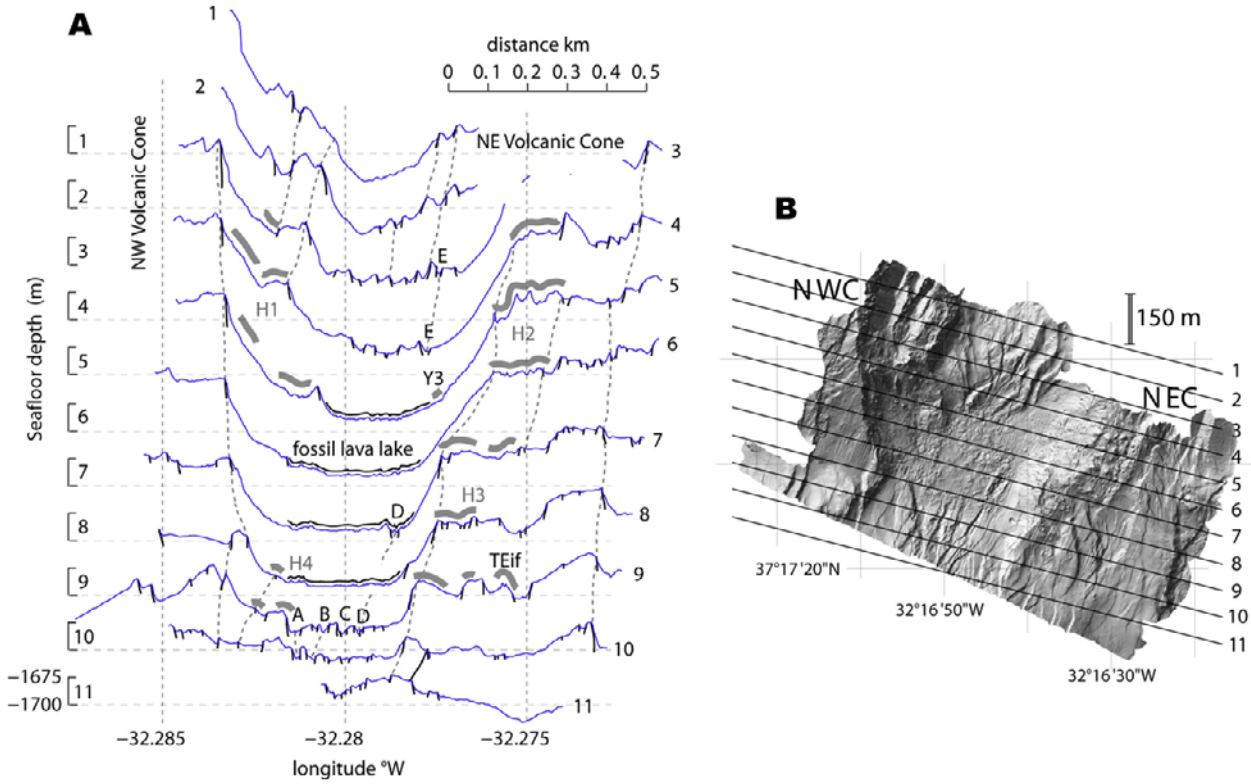

Figure 5. (a) Ridge-perpendicular sections across the area mapped by the MMR tool and (b) sections located on shaded high-resolution bathymetry. Vertical exaggeration is 3.5 times. Grey lines above bathymetry show extent of inferred hydrothermal areas (as in Figure 4). H1, H2, H3, and H4 are hydrothermal areas discussed in text. Short black lines are inferred faults, and fissure walls, corresponding to the scarps visible in the bathymetry. NWC: Northwest Volcanic Cone; NEC: Northeast Volcanic Cone. TEif for Tour Eiffel vent.

5.1.2. NE Hydrothermal Venting Area

[19] The NE hydrothermal venting area (H2 in Figure 4) includes two known active vents (Sintra and Statue of Liberty; Figure 3a). It extends some ~180 m by 220 m on a shelf that forms the southwestern part of the Northeastern Volcanic Cone (Figure 5, sections 4 to 6). This shelf is limited to the west by a steep slope made of talus of hydrothermal sulfides as seen during dives, going down some 100 m to the fossil lava lake. This slope is the southward continuation of the steep NNE-trending and linear scarp that bounds the Northeast Volcanic cone to the west (Figure 2a). We infer that the somewhat irregular slope next to the NE vents formed by mass wasting of this fault scarp. The NE hydrothermal venting area has a roughly rectangular shape, being limited to the east by a NNE-trending and east-facing scarp and to the south by a smaller, WNW-trending and south-facing scarp (Figure 4). Both of these scarps are about 10 m high and end abruptly at their intersection, at the southeastern corner of venting area H2. The lumpy and spiky seafloor morphology is particularly well developed in this NE venting area. Dive observations reveal that it comprises numerous extinct sites, with large blocks of broken chimneys and prominent sulfide mounds, 15 to 25 m in diameter and 8 to 15m high (Figures 4b and 4c).

5.1.3. SE Hydrothermal Area

[20] The SE hydrothermal area (H3 in Figure 4) is located on the saddle between the southern volcanic cone and the northeastern volcanic cone (Figures 2a and 3a). The new bathymetric data coupled with submersible observations show that the vents are built on hydrothermally cemented volcanic breccia that is refered to as the "slab" (Figure 4f), and that the surrounding seafloor is sedimented and cut by a dense network of fissures and scarps. These scarps trend NNE to NNW and are up to 10–12 m high (Figures 2b, 3a, 4, and 5, sections 8 to 10). Many are curvilinear and concave to the west. The SE hydrothermal venting area includes the largest number of known active vents at Lucky Strike, forming five subgroups, each surrounded by a

relatively small area (30 to 60 m across) of lumpy seafloor visible on the new bathymetric data (PP4, Isabel, Chimiste, Tour Eiffel, and the Montsegur, U.S.4, U.S.6 and U.S.7; Figure 3a). A sixth area of lumpy seafloor, with no known active vent, occurs about 100m to the south of Isabel (Figures 3a and 4).

5.1.4. SW Hydrothermal Area

[21] The SW hydrothermal venting area (H4 in Figure 4) includes at least three and possibly five distinct active vent sites (Nuno, Hélène, White Castle, Pico, and Crystal). It extends some 100 m by 100 m in the heavily fissured terrain across the SE shore of the fossil lava lake (Figures 3a, 4, and 5, sections 8 and 9). According to dive observations, the Pico vent lies at the summit of a 20 m-high, NNE-trending, and east facing scarp that forms the local limit of the fossil lava lake and extends some 50 m to the south (Figure 3a). White Castle and Crystal may similarly be associated with a rectilinear scarp that trends NNE over at least 200 m (Figure 3a), with a heave of only 6 m. Contrary to vents in areas H1, H2, and H3, the H4 vents are not associated with visible domains of lumpy seafloor on the new bathymetric map. The different sites of this area, visited by submersible, may correspond in our bathymetric data with small spikes at the limit of resolution (Figures 3a and 4). Nuno, located on the shore of the lava lake (Figure 4e) is an active site expelling a 175°C fluid. Most discharges are diffusive though barite and sphalerite dominant chimneys up to 5 m high (Y. Fouquet, personal communication, 2008). Submersible dives south of Nuno have also documented inactive and partly oxidized chimneys near the shore of the lava lake. The bases of these chimneys are partly buried under the most recent lava flows. The Helene site is a group of active and inactive chimneys set on the lava lake formations.

5.2. Fossil Lava Lake and the Surrounding Fissure Network

[22] The fossil lava lake fills the nearly circular depression between the three summit volcanic cones of the Lucky Strike volcano. The new high-resolution data allows us to resolve the contours of this lake with a precision of a few meters. The clearest image comes from reverse backscatter data (Figure 3b): the ropy and lightly sedimented lava in the lake is less reflective than the surrounding formations of basalt talus and hydrothermal deposits. In situ observations confirm that these facies are associated with glassy and lightly sedimented recent lavas [*Ondréas et al.*, 1997]. These dive observations show that the freshest lava in the hydrothermal area are found in the lava lake and that lobate lava locally flow out of the lake on the layered volcaniclastic material. In situ observations also indicate an absence of lobate lava on the three volcanic cones where only volcaniclastic material and pillow lava are observed.

[23] The outer contour of the fossil lava lake, corresponding to the limit of the low/high backscatter signal, probably represents the level of maximum filling of the lake. It corresponds almost exactly with the 1734 m isobath (Figures 6a and 6d), except in the southwestern corner of the lake, where it is depressed by about 2.5 m (Figure 6a). In this depressed area, close to the H4 hydrothermal vents (Figure 4), the lake contour follows the foot of a NW-trending, east-facing, 20 m high scarp. We infer that this scarp corresponds to a normal fault which has moved since the lake was last active. The lake contour also occasionally differs from the 1734 m isobath in small V-shaped indentations, many of which correspond to fissures in the terrains surrounding the lake (Figure 6a).

[24] The lava lake has a surface area of 95,000 m^2. It extends about 320 m from west to east and 350 m from north to south. Careful examination of the backscatter data revealed no evidence for fresh lavas outside the lake. We therefore rule out the possibility that the lake represents a lava-filled depression fed by external eruptive vents. The shaded bathymetry map of the lake (Figure 6b) shows three distinct volcanic morphologies, which have been ground-truthed by dive observations: ropy, flat, and hummocky. The hummocky morphology corresponds to collapsed lobate lavas and pillars and is mostly found in the periphery of the lake, where layered sheet flows have been observed [*Ondréas et al.*, 1997]. Dive observations suggest that the flat morphology corresponds to sheet flows with a light dusting of sediments. Finally, the ropy morphology corresponds to non-collapsed lobate lavas and to draped lava flows [cf. *Ondréas et al.*, 1997, Figure 6b]. Circular spikes can also be identified on the slope map (Figure 6c). They correspond to lava pillars, and to occasional inactive hydrothermal edifices, which can both reach 6 m in height (Figure 4e). The pillars exhibit regularly spaced shelves of lava. By analogy with similar structures observed at intermediate or fast spreading ridges [*Francheteau et al.*, 1979; *Gregg and Chadwick*, 1996; *Gregg et al.*, 2000; *Chadwick*, 2003], we interpret these lava shelves as

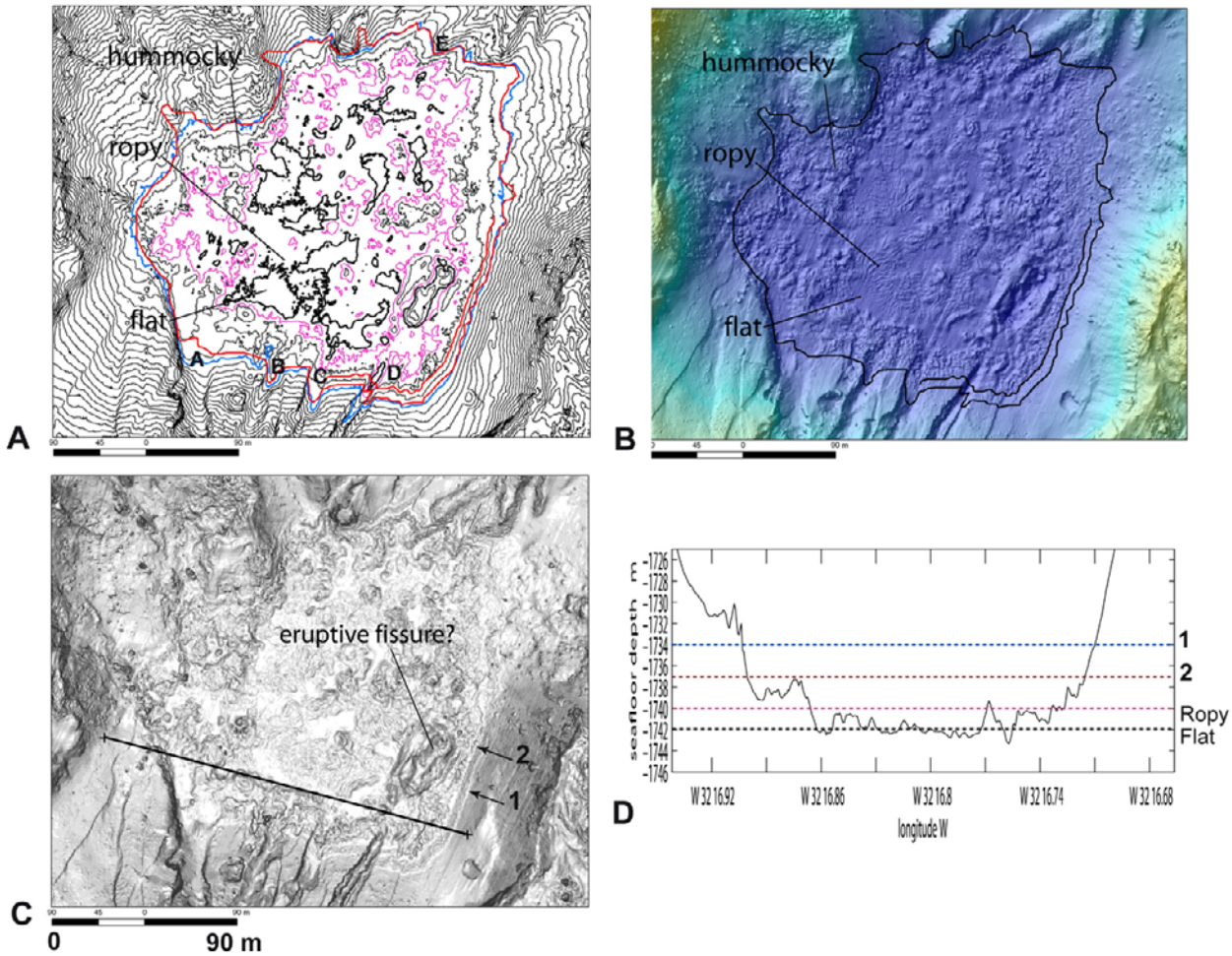

Figure 6. Detail of high-resolution MMR survey showing the lava lake area. (a) Contour map with isobaths spaced at 2 m. Outer red contour is the limit of the lava lake as in Figure 3; inner red contour is the level of drainback as seen on slope map. Pink isobath is 1740 m; thick black isobath is 1742 m; blue isobath is 1734 m. Hummocky, ropy and flat refer to lava morphologies described in text. (b) Shaded bathymetry (as in Figure 2). Outer black contour is the limit of the lava lake as in Figure 3; inner black contour is the level of drainback as seen on slope map. (c) Slope map (as in Figure 3). The numerals "1" and "2" refer to the two slope breaks which we infer mark successive levels of drainback of the lava lake (see text). (d) Cross section located in Figure 6c and corresponding to the center part of section 8 in Figure 5. Colors correspond to the isobaths shown in Figure 6a. Vertical exaggeration is 10 times.

formed during draining events during the period of activity of the lake.

[25] The flat morphologies are found in the deepest areas of the lake. They correspond very nearly to the 1742 m isobath, while the contours of ropy morphologies correspond nicely with the 1740 m isobath (Figures 6a and 6d). We infer that these ropy morphologies correspond to the latest eruptive event, after the end of the lava lake formation. During this event, lobate flows and draped lava were emplaced, which did not cover the whole surface of the former lake. The flat morphologies, which are the deepest, would then correspond to areas of the former lake that were not recovered by lobate flows and draped lava. The 8 m difference between the 1742 m and the 1734 m isobaths most likely represents the drop of the level in the lake before it froze. The maximum height of lava pillars, as estimated from submersible observations [*Fouquet et al.*, 1995a], is consistent with this interpretation. Along the southeastern and southern shores of the lake, the slope map (Figure 6c) shows a small, yet distinct slope break at 1737 m. This slope break is also visible locally along the northern shore of the fossil lake (Figure 6c). We infer that it is not visible elsewhere because the terrains along the lake's shores are too steep and/or too rough. We propose that this shelf, which corresponds to a 3 m drop in the level of the lake, represents an

intermediate stage during the emptying of the lake before it froze.

[26] Although the seafloor topography in the fossil lake is rough, it appears to be the result of lava collapse, and there is only limited evidence for faulting or fissuring. By contrast, the surrounding seafloor, particularly to the north and to the south, is clearly tectonized, with meter- to decameter-wide fissures and fault scarps, most of which trend N20 to N30, perpendicular to plate divergence (Figures 2a; Figure 5, sections 2, 3, 4, and 9, 10, 11; Figures 6b and 6c). These fissures and scarps are concentrated in the NNE-trending axial zone, as defined by *Scheirer et al.* [2000]. This zone of recent tectonics is 300 to 400 m in width. It runs between the Northwest and Northeast Volcanic cones and cuts to the south through the South Cone (Figure 2a).

[27] There are four mains fissures in this axial zone south of the fossil lava lake. Fissure A (Figure 6a) is the largest, with a width of 20 m and a depth of 15 m (Figure 5, sections 9 and 10). It extends at least 150 m from the lake's shore southward. The lake's upper contour does not follow the indented 1734 m isobath near this fissure, but is instead depressed by 2 to 3 m, indicating that fissure A formed after the lava had retreated below this level. By contrast, the lake's contour is indented and coincides with the 1734 m isobaths near fissures B and C (Figure 6a). This indicates that these 10 to 12 m wide and 5 to 8 m deep fissures (Figure 5, sections 9 and 10) predated the period of maximum filling of the lava lake. Fissure D (Figure 6a) is a more complex case: it clearly deforms the lake's contour and can be followed into the lake for some 50 m. It then disappears for another few tens of meters, buried in lavas with a hummocky morphology, and reappears in the form of a broad fissure with two adjacent elongated ridges (Figure 6 and Figure 5, section 7). This portion of fissure D, however, does not have scarps with sharp edges as it does further to the south. Our interpretation is that fissure D was active soon after the lake had frozen, and served as an eruptive fissure during the later stages of volcanic activity in the lake area. We interpret the two elongated ridges adjacent to the fissure in the lake, as volcanic constructions formed during these later stages.

[28] The terrain to the north of the fossil lake is also fissured, but the highest scarps there do not have sharp edges, suggesting that they may be partly buried in lava and sediment. The deepest and widest fissure (E in Figure 6; Figure 5, sections 3 and 4) is 16 m wide and 12 m deep. The contour of the lava lake follows closely the indentations of the 1734 m isobath near these fissures, indicating that they predate the period of maximum filling of the lava lake.

6. Discussion

6.1. Distribution of Hydrothermal Venting at Lucky Strike

[29] Massive sulfides, producing chaotic and lumpy seafloor morphologies, are widespread in the NW (H1) and NE (H2) hydrothermal areas (Figure 4). From this we infer that hydrothermal venting there has been going on for quite some time, allowing for substantial volumes of sulfides to accumulate. The NW (H1) area is smaller but more active as of the last dives in the area which we reexamined for this paper (IRIS cruise, 2001) than the NE (H2) area. Both are located 50 to 130 m above the level of the lava lake, near the large scarps which bound the Northwest and the Northeast Volcanic cones. The NE (H2) venting area is located on a shelf above the eastern scarp (Figure 5). The NW (H1) venting area is set on sulfide talus that covers the eastern slope of the Northwest Volcanic Cone. This slope, which is about 130 m high, has a sharp and curvilinear upper scarp (Figures 4 and 5), which we interpret as the scar of a landslide. If this interpretation is correct, the NW hydrothermal area (H1) may originally have been located in the footwall side of one of the axial graben normal faults, in a setting symmetrical to that of the NE hydrothermal area (Figure 7A).

[30] The SE hydrothermal sites (H3 in Figures 4 and 5) lie on top of tectonized slabs of hydrothermally cemented and silicified volcanic breccia, in the southern continuation of the shelf that also hosts the NE (H2) vent sites. On the basis of the distribution of lumpy seafloor morphologies, it appears that these SE hydrothermal deposits are dominantly vertical chimneys with scarce massive sulfide deposits. The high-resolution map also shows that the SE sites are located on or near crosscutting fault scarps (Figure 3). Silica precipitated within the layered volcanoclastic (Figure 4g) probably sealed permeability in the slab formation [*Humphris et al.*, 2002], constraining fluid to escape from these crosscutting faults.

[31] Finally, the SW vent sites (H4 in Figures 4 and 5) have not built hydrothermal deposits sufficient to be visible in the high-resolution map.

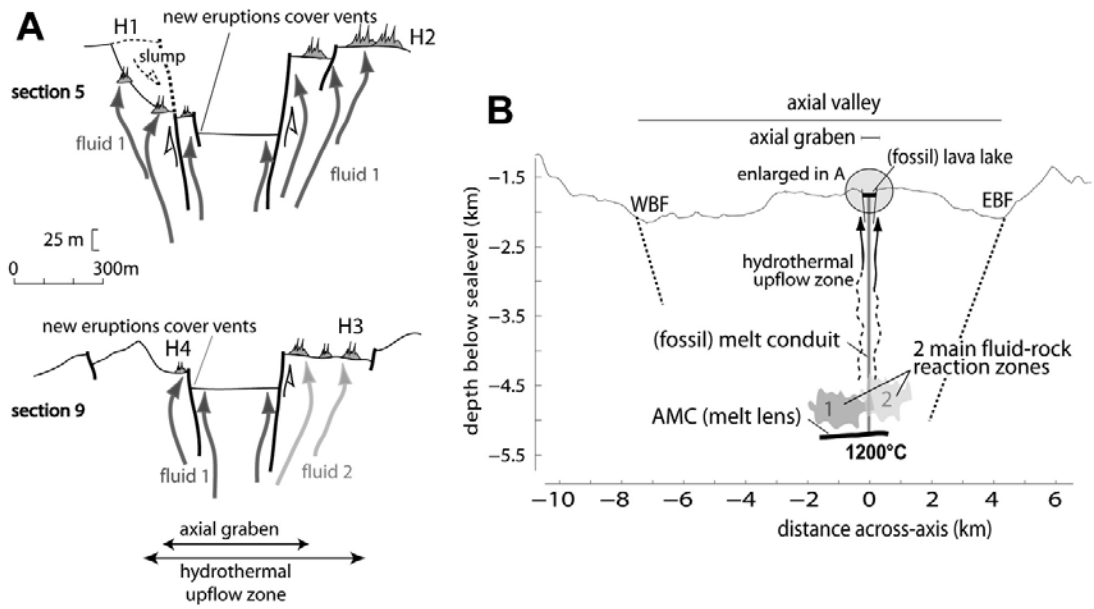

Figure 7. (a) Interpretative sketches drawn for cross sections 5 and 9 of Figure 5. Vents in the H1 and H2 groups are set in the footwall of the axial graben bounding faults (H1 is now set in talus formed by gravitational collapse of the fault scarp, shown in dashed line and arrow). We infer that these sites have been tectonically uplifted above the level of most axial eruptions for long enough to build large sulfide deposits. By contrast, vents in the H4 group grow on recent lava flows, recently faulted above the bottom level of the graben. These vents have not yet built significant sulfide mounds. Vents in the H3 group are built on the slab of silicified volcaniclastic deposits and are in an intermediate setting. Fluids discharging at group H3 appear distinct from those of the groups H1, H2, and H4 [*Von Damm et al.*, 1998; *Charlou et al.*, 2000]. (b) Across-axis section (located in Figure 1) through the center of the Lucky Strike central volcano, showing the depth and width of the axial magma chamber seismic reflector (AMC) [*Singh et al.*, 2006] and the two axial valley bounding faults (West Bounding Fault and East Bounding Fault; the EBF is drawn as imaged in seismic reflection record [*Combier et al.*, 2007]). Also shown are the smaller faults which bound the axial graben, where most recent tectonic and volcanic activity takes place. The lava lake is inferred to have been connected to the AMC by an open conduit, during its period(s) of activity. The two main fluid-rock reaction zones, and the hydrothermal upflow zone are also sketched (see discussion in text).

With the exception of the Helene site, which is built on the lava lake, the SW sites are built on partly silicified volcaniclastic formations, similar to the SE sites. They are set on the southern shore of the fossil lava lake and are associated with NNE-trending scarps and fissures (Figure 3). We show that the widest of these fissures at least (labeled A in Figures 5 and 6) formed after the lava lake was frozen. *Humphris et al.* [2002] report a "lack of hydrothermal activity within the lava lake itself because recent lava flows provide a barrier to upflowing fluids." However, the Nuno site is located near the shore of the lake, on recent lava, and the Helene site is located on the lake itself. These sites are therefore younger than the lava lake. Inactive and partly oxidized chimneys near the Nuno site have also been observed during previous dives to be partly buried under the most recent lava flows. From this we infer that hydrothermal activity in this SW area has persisted through at least recent eruptive episodes. We also infer that Nuno, and the other sites in the SW hydrothermal area, are presently controlled by recent faults formed near the western shore of the lava lake.

[32] The study of the high-resolution bathymetric data in the perspective of previous dive observations permits us to propose a gradation in the apparent age of vents in the Lucky Strike hydrothermal field. The two groups of sites which presently lie well above the bottom of the axial graben (H1 and H2; Figure 7a) appear to have been active for the longest duration. By contrast, vents which are deeper, and closer to the lava lake (H4 and the isolated site Y3), are frequently buried by new lava flows, so that, even if venting there does resume after the eruption, the site will appear young based on the size of associated deposits. The SE sites (H3) are located on the slab formation and also appear to be young based on the size of visible hydrothermal deposits. We infer that they

formed after faulting created new pathways for fluids in the volcaniclastic material which was deposited over this area [*Fouquet et al.*, 1998], then cemented by silica which precipitated from cooler and diffuse fluid circulations. This leads us to propose that the size (and apparent age) of hydrothermal deposits in the Lucky Strike vent field is primarily controlled not by possible complexities of the hydrothermal upflow zone at depth, but by the age of the eruptive events which may have covered preexisting sulfide deposits at each site, and/or by the age of the tectonic events which reactivated fluid pathways beneath each of these sites. We infer that the northern vent sites (H1 and H2) presently have large sulfide deposits because they have been tectonically uplifted well above the level of most axial eruptions (Figure 7a).

[33] *Humphris et al.* [2002] have proposed a model for the tectonic, volcanic, and hydrothermal interactions at Lucky Strike Seamount in which they invoke volcano-tectonic cycles and sealing of the system by silicified hydrothermal slab formations to explain the distribution of hydrothermal activity. We do not focus our interpretation on possible volcano-tectonic cycles; however, we confirm that the distribution of outcropping hydrothermal deposits and active sites at Lucky Strike is controlled by volcanism (the extent of eruptive events) and tectonics (the distribution of faults). We also confirm that high temperature hydrothermal circulations have been focused for a long period of time at the summit of the Lucky Strike volcano, creating the lumpy terrains in the NW and NE hydrothermal areas. Finally, we identify a recent phase of faulting and fracturing of the SW part of the lava lake, providing access to hydrothermal fluids, and allowing vents to grow on the freshest ropy lava.

[34] The distribution of present-day vents indicates that the hydrothermal upflow zone beneath the Lucky Strike vent field is wider than the axial graben, where most eruptions initiate (Figures 7a and 7b). Differences in the end-member compositions of fluids between the SE vents and the other vents [*Langmuir et al.*, 1997; *Von Damm et al.*, 1998, Charlou et al. 2000] indicate the need for two different sources. This suggests that the hydrothermal upflow zone feeds at least two distinct water-rock reaction zones at depth. At present, there are no constraints available as to the nature of these reaction zones. In Figure 7b, we infer that they are located above the melt lens imaged at 3 to 4 km bsf by *Singh et al.* [2006].

6.2. Lucky Strike Lava Lake

[35] Since the initial descriptions of the Lucky Strike segment by *Fouquet et al.* [1995a] and *Langmuir et al.* [1997], the semicircular expanse of flat and ropy lavas in the center of the Lucky Strike volcano has been described as a lava lake. Our observations confirm that this lake was not fed by external eruptive vents. The existence of a bench, and of lava pillars, which we interpret as evidence for drainback, indicates this volcanic feature did, over its period of activity, connect to a melt reservoir through an open conduit. In the interpretative sketch shown in Figure 7b, we propose that the melt reservoir corresponds to the body of melt presently documented seismically 3 to 4 km beneath the Lucky Strike volcano [*Singh et al.*, 2006].The lack of fissures and fractures in the new high-resolution bathymetry of the lake surface is a confirmation that it drained and froze recently. The present configuration of the lake, with its flat drained-back surface, its lava pillars and its local accumulations of draped lavas, which we infer erupted from fissure D (Figures 5 and 6) and form the most recent eruptive products on the lake surface, only informs us on the last stages of its activity. We therefore have no evidence to constrain the duration of the lake's activity. It may well have been short (a few days, or a single axial eruption), the open conduit being simply the dike feeding the eruption. The lava accumulated in the depression between the three summits cones and covered the eruptive vents. In this case, the lake should probably better be referred to as a lava pond. Alternatively, the lake's activity may have lasted longer, implying a different formation mechanism, with a longer lasting hydraulic connection to the magma chamber, as documented for lava lakes on land [e.g., *Witham and Llewellin*, 2006].

[36] The Lucky Strike lava lake contains flat lavas and lava pillars similar to those observed at the axis of the intermediate and fast spreading ridges [*Ballard*, 1979; *Francheteau et al.*, 1979; *Auzende et al.*, 1996; *Gregg and Chadwick*, 1996; *Gregg et al.*, 2000; *Lagabrielle et al.*, 2001; *Chadwick*, 2003; *Tanaka et al.*, 2007]. Lava pillars have also been reported at the Mid-Atlantic Ridge south of the Oceanographer transform [*Bideau et al.*, 1998]. The lava pillars at Lucky Strike are smaller, up to 6 m, compared to those described on the East Pacific Rise (EPR) reaching 10 to 20 m in high [*Francheteau et al.*, 1981; *Auzende et al.*, 1996]. They present selvages and glassy tops similar to those of the EPR pillars [*Francheteau et al.*, 1981].

Shelves on lava pillars at Mid-Ocean Ridges have been shown to form when lava drains out, and their spacing and thickness is inferred to be related to the rate of this drainback [*Chadwick*, 2003]. The pressure gauge of a seismometer caught in a lava flow at the Juan Fuca Ridge has provided the first quantitative constraints on the timescale of lava pillar formation and on the rate of drainback of a submarine lava flow: 3.5 m of drainback in 2.5 h [*Fox et al.*, 2001; *Chadwick*, 2003]. The spacing and the thickness of the pillar's shelves on Lucky Strike (5–10 cm of spacing and 1–2 cm of thickness; Y. Fouquet, personal communication, 2008) are the same than those described on the EPR by *Gregg et al.* [2000], suggesting that the drainback of the lake may have occurred at a similar rate.

[37] Lava drainback at Lucky Strike is also marked by a bench visible along the southeastern shore of the lava lake (Figure 6). Similar volcanic features have been described in collapsed lava ponds of the EPR [*Francheteau et al.*, 1981; *Haymon et al.*, 1991; *Auzende et al.*, 1996; *Lagabrielle et al.*, 2001; *Chadwick*, 2003; *Tanaka et al.*, 2007], and interpreted to reflect draining of the lava out of the axial through, or back down the eruptive vents. The main features of the Lucky Strike lava lake are therefore similar to those of lava lakes, or lava ponds, at faster spreading ridges.

7. Conclusions

[38] On the basis of new high-resolution bathymetry and seafloor reflectivity data for the summit of the Lucky Strike volcano, and on observations previously made during numerous dives in the area, we have refined the spatial distribution of hydrothermal edifices. We provide new constraints on the recent history of hydrothermal venting and eruptive activity at Lucky Strike. These observations suggest a complex recent eruptive activity, starting with eruptions of a gas-rich magma [*Langmuir et al.*, 1997; *Ferreira et al.*, 2005], which produced the autobrecciated volcaniclastic material and the highly vesicular lava observed on the three summit volcanic cones [*Ondréas et al.*, 1997; *Fouquet et al.*, 1998; *Eissen et al.*, 2003]. Sulfide edifices in the NW and NE hydrothermal areas initiated their growth after this eruptive episode, while cooled hydrothermal fluids precipitated silica in the volcaniclastic deposits next to the central depression, forming an impermeable slab [*Humphris et al.*, 2002]. The lava lake was then formed, producing degassed lava flows which poured locally on the volcaniclastic formation, and on successive generations of short-lived chimneys built along the edge of the lava lake. The activity of the lake is the most recent eruptive event detected at Lucky Strike. Lava drainback is evidenced by benches and lava pillars, and suggest a close connection with an underlying magma reservoir, which we infer corresponded to the melt body imaged by *Singh et al.* [2006]. We have found no evidence that this lake was active for months to decades, as lava lakes at terrestrial volcanoes [*Tazieff*, 1984; *Tilling*, 1987]. It may instead have formed as a lava pond, with successive lava flows covering the eruptive vents, as proposed for similar features at the EPR. The horizontal surface of the lake is deformed only near its southwestern shore, along a NNE-trending set of faults and fissures, which appear to control the distribution of hydrothermal chimneys.

[39] The distribution of exposed sulfide deposits and active vents within the Lucky Strike field is consistent with a wide hydrothermal upflow zone. We infer that this upflow zone roots into a complex system of melt-rock reaction zones located above the melt lens imaged by seismic methods at depths of 3 to 4 km beneath the volcano. We also propose that the present-day distribution of exposed hydrothermal deposits and active vents at Lucky Strike is controlled by the spatial distribution of eruptive products which may have covered preexisting sulfide deposits and by the faults which provide reactivated pathways for hydrothermal fluids.

Acknowledgments

[40] We thank the captain and the crew of the R/V *Pourquoi Pas?*, the team which operates the ROV *Victor,* and the shipboard scientists of the MoMAReto cruise for collecting the high-resolution multibeam data. Special thanks to Patrick Siméoni, the engineer in charge of the *Victor* MMR. Jean-Marc Sinquin, Eliane Le Drezen, and Anne-Sophie Alix helped with processing of the microbathymetry and backscatter data. We thank Anne Godfroy, chief scientist of the EXOMAR cruise. We also thank Susan Humphris and one anonymous reviewer for their constructive and detailed reviews. The MoMAReto cruise was partly funded by the EXOCET/D European project, contract GOCE-CT-2003-505342. This is IPGP contribution 2435.

References

Auzende, J. M., et al. (1996), Recent tectonic, magmatic, and hydrothermal activity on the East Pacific Rise between 17 degrees S and 19 degrees S: Submersible observations, *J. Geophys. Res.*, *101*(B8), 17,995–18,010, doi:10.1029/96JB01209.

Ballard, R. D. (1979), The Galapagos Rift at 86°W: Sheet-flows, collapse pits and lava lakes of the rift valley, *J. Geophys. Res.*, *84*, 5407–5422, doi:10.1029/JB084iB10p05407.

Bideau, D., R. Hekinian, B. Sichler, E. Gracia, C. Bollinger, M. Constantin, and C. Guivel (1998), Contrasting volcanic-tectonic processes during the past 2 Ma on the Mid-Atlantic Ridge: Submersible mapping, petrological and magnetic results at lat. 34°52′N and 33°55′N, *Mar. Geophys. Res.*, *20*, 425–458, doi:10.1023/A:1004760111160.

Cannat, M., et al. (1999), Mid-Atlantic Ridge–Azores hotspot interactions: Along-axis migration of a hotspot-derived event of enhanced magmatism 10 to 4 Ma ago, *Earth Planet. Sci. Lett.*, *173*(3), 257–269.

Chadwick, W. W. (2003), Quantitative constraints on the growth of submarine lava pillars from a monitoring instrument that was caught in lava flow, *J. Geophys. Res.*, *108*(B11), 2534, doi:10.1029/2003JB002422.

Chadwick, W. W., D. S. Scheirer, R. W. Embley, and H. P. Johnson (2001), High-resolution bathymetric surveys using scanning sonars: Lava flow morphology, hydrothermal vents, and geologic structure at recent eruption sites on the Juan de Fuca Ridge, *J. Geophys. Res.*, *106*(B8), 16,075–16,099, doi:10.1029/2001JB000297.

Charlou, J. L., J. P. Donval, E. Douville, P. Jean-Baptiste, J. Radford-Knoery, Y. Fouquet, A. Dapoigny, and M. Stievenard (2000), Compared geochemical signatures and the evolution of Menez Gwen (37 Deg50′N) and Lucky Strike (37 Deg17′N) hydrothermal fluids, south of the Azores Triple Junction on the Mid-Atlantic Ridge, *Chem. Geol.*, *171*(1–2), 49–75, doi:10.1016/S0009-2541(00)00244-8.

Chen, Y. J. (1992), Oceanic crustal thickness versus spreading rate, *Geophys. Res. Lett.*, *19*, 753–756, doi:10.1029/92GL00161.

Combier, V., T. Seher, S. Singh, W. Crawford, H. Carton, M. Cannat, and J. Escartin (2007), Three-dimensional geometry of magma chamber roof and faults from 3D seismic reflection data at the Lucky Strike volcano, Mid-Atlantic Ridge, *Geophys. Res. Abstr.*, *9*, A-03062.

Cormier, M. H., W. B. F. Ryan, A. K. Shah, W. Jin, A. M. Bradley, and D. R. Yoerger (2003), Waxing and waning volcanism along the East Pacific Rise on a millennium time scale, *Geology*, *31*(7), 633–636, doi:10.1130/0091-7613(2003)031<0633:WAWVAT>2.0.CO;2.

DeMets, C., R. G. Gordon, D. F. Argus, and S. Stein (1990), Current plate motions, *Geophys. J. R. Astron. Soc. London*, *101*, 425–478.

Detrick, R. S., H. D. Needham, and V. Renard (1995), Gravity anomalies and crustal thickness variations along the Mid-Atlantic Ridge between 33°N and 40°N, *J. Geophys. Res.*, *100*, 3767–3787, doi:10.1029/94JB02649.

Dosso, L., H. Bougault, C. Langmuir, C. Bollinger, O. Bonnier, and J. Etoubleau (1999), The age and distribution of mantle heterogeneity along the Mid-Atlantic Ridge (31–41°N), *Earth Planet. Sci. Lett.*, *170*, 269–286, doi:10.1016/S0012-821X (99)00109-0.

Edwards, M. H., G. J. Kurras, M. Tolstoy, D. R. Bohnenstiehl, B. J. Coakley, and J. R. Cochran (2001), Evidence of recent volcanic activity on the ultraslow-spreading Gakkel ridge, *Nature*, *409*, 808–812, doi:10.1038/35057258.

Eissen, J. P., Y. Fouquet, D. Hardy, and H. Ondréas (2003), Recent MORB volcaniclastic explosive deposits formed between 500 and 1750 m.b.s.l. on the axis of the Mid-Atlantic Ridge, south of the Azores, in *Explosive Subaqueous Volcanism*, *Geophys. Monogr. Ser.*, vol. 140, edited by J. D. L. White et al., pp. 143–166, AGU, Washington, D. C.

Escartin, J., M. Cannat, G. Pouliquen, A. Rabain, and J. Lin (2001), Crustal thickness of V-shaped ridges south of the Azores: Interaction of the Mid-Atlantic Ridge (36°–39°N) and the Azores hot spot, *J. Geophys. Res.*, *106*(B10), 21,719–21,735, doi:10.1029/2001JB000224.

Ferreira, P. L., B. J. Murton, and C. Boulter (2005), Mixing two enriched and distinct mantle sources beneath Lucky Strike segment, 37 degrees N on the Mid-Atlantic Ridge, *Geochim. Cosmochim. Acta*, *69*(10), A102.

Fornari, D., et al. (1996), Detailed studies of the Lucky Strike Seamount based on DSL-120 sonar, ARGO II and ROV Jason studies, *Eos Trans. AGU.*, *77*(46), Fall Meet. Suppl., F699.

Fouquet, Y., J. L. Charlou, J. P. Donval, J. Knoery, H. Pelle, H. Ondréas, M. Segonzac, I. Costa, N. Lourenço, and M. K. Tivey (1995a), DIVA1 cruise: Geological control and composition of hydrothermal deposits near the Azores Triple Junction, *Terra Nova*, *7*, 211.

Fouquet, Y., H. Ondréas, J. L. Charlou, J. P. Donval, J. Radfort-Knoery, I. Costa, N. Lourenço, and M. K. Tivey (1995b), Atlantic lava lakes and hot vents, *Nature*, *377*, 201, doi:10.1038/377201a0.

Fouquet, Y., J. P. Eissen, H. Ondréas, F. Barriga, R. Batiza, and L. Danyushevsky (1998), Extensive volcaniclastic deposits at the Mid-Atlantic Ridge axis: Results of deep-water basaltic explosive volcanic activity?, *Terra Nova*, *10*(5), 280–286, doi:10.1046/j.1365-3121.1998.00204.x.

Fox, C. G., W. W. Chadwick, and R. W. Embley (2001), Direct observations of a submarine volcanic eruption from the seafloor instrument caught in a lava flow, *Nature*, *412*, 727–729, doi:10.1038/35089066.

Francheteau, J., T. Juteau, and C. Rangin (1979), Basaltic pillars in collapsed lava-pools on the deep ocean floor, *Nature*, *281*(5728), 209–211, doi:10.1038/281209a0.

Francheteau, J., et al. (1981), First manned submersible dives on the East Pacific Rise at 21°N (PROJECT RITA) - General results, *Mar. Geophys. Res.*, *4*, 345–379, doi:10.1007/BF00286034.

Gregg, T. K., and W. W. Chadwick (1996), Submarine lava-flow inflation: A model for the formation of lava pillars, *Geology*, *24*(11), 981–984, doi:10.1130/0091-7613(1996)024<0981:SLFIAM>2.3.CO;2.

Gregg, T. K., D. J. Fornari, M. R. Perfit, W. I. Ridley, and M. D. Kurz (2000), Using submarine lava pillars to record mid-ocean ridge eruption dynamics, *Earth Planet. Sci. Lett.*, *178*(3–4), 195–214, doi:10.1016/S0012-821X(00)00085-6.

Haymon, R. M., D. J. Fornari, M. H. Edwards, S. Carbotte, D. Wright, and K. C. Macdonald (1991), Hydrothermal vent distribution along the East Pacific Rise crest (9°09′–54′N) and its relationship to magmatic and tectonic processes on fast-spreading mid-ocean ridges, *Earth Planet. Sci. Lett.*, *104*, 513–534, doi:10.1016/0012-821X(91)90226-8.

Humphris, S. E., and M. C. Kleinrock (1996), Detailed morphology of the TAG active hydrothermal mound: Insights into its formation and growth, *Geophys. Res. Lett.*, *23*, 3443–3446, doi:10.1029/96GL03079.

Humphris, S. E., D. J. Fornari, L. M. Parson, and C. R. German (1996), Geologic and tectonic setting of hydrothermal activity on the summit of Lucky Strike seamount (37°17′N) (Mid-Atlantic Ridge), *Eos Trans. AGU.*, *77*, *46*, Fall Meet. Suppl., F699.

Humphris, S. E., D. Fornari, D. Scheirer, C. R. German, and L. M. Parson (2002), Geotectonic setting of hydrothermal activity on the summit of Lucky Strike Seamount (37°17′N) (Mid-Atlantic Ridge), *Geochem. Geophys. Geosyst.*, *3*(8), 1049, doi:10.1029/2001GC000284.

Kurras, G. S., M. H. Edwards, and D. J. Fornari (1998), High-resolution bathymetry of the East Pacific Rise axial summit trough 9°49′–51′N: A compilation of Alvin scanning sonar

and altimetry data from 1991–1995, *Geophys. Res. Lett.*, *25*(8), 1209–1212, doi:10.1029/98GL00721.

Lagabrielle, Y., E. Garel, O. Dauteuil, and M.-H. Cormier (2001), Extensional faulting and caldera collapse in the axial region of fast spreading ridges: Analog modeling, *J. Geophys. Res.*, *106*(B2), 2005–2015, doi:10.1029/2000JB900266.

Langmuir, C. H., et al. (1993), Geological Setting and characteristics of the Lucky Strike vent field at 37°17N on the Mid-Atlantic Ridge, *Eos Trans. AGU.*, *74*(43), Fall Meet. Suppl., F99.

Langmuir, C., et al. (1997), Hydrothermal vents near a mantle hot spot: The Lucky Strike vent field at 37°N on the Mid-Atlantic Ridge, *Earth Planet. Sci. Lett.*, *148*, 69–91, doi:10.1016/S0012-821X(97)00027-7.

Miranda, J. M., J. F. Luis, N. Lourenco, and F. M. Santos (2005), Identification of the magnetization low of the Lucky Strike hydrothermal vent using surface magnetic data, *J. Geophys. Res.*, *110*, B04103, doi:10.1029/2004JB003085.

Ondréas, H., Y. Fouquet, M. Voisset, and J. Radford-Knoery (1997), Detailed Study of three contiguous segments of the Mid-Atlantic Ridge, south of the Azores (37°N to 38°30N), using acoustic imaging coupled with submersible observations, *Mar. Geophys. Res.*, *19*, 231–255, doi:10.1023/A:1004230708943.

Parson, L., E. Gracia, D. Coller, C. German, and D. Needham (2000), Second-order segmentation; the relationship between volcanism and tectonism at the MAR, 38°N–35°40′N, *Earth Planet. Sci. Lett.*, *178*, 231–251, doi:10.1016/S0012-821X(00)00090-X.

Sarrazin, J., P. M. Sarradin, and the MOMARETO participants (2006), MOMARETO: A cruise dedicated to the spatio-temporal dynamics and the adaptations of hydrothermal vent fauna on the Mid-Atlantic Ridge, *InterRidge News*, *15*, 24–33.

Scheirer, D. S., D. J. Fornari, S. E. Humphris, and S. Lerner (2000), High-resolution seafloor mapping using the DSL-120 sonar system: Quantitative assessment of sidescan and phase-bathymetry data from the Lucky Strike segment of the Mid-Atlantic Ridge, *Mar. Geophys. Res.*, *21*, 121–142, doi:10.1023/A:1004701429848.

Seher, T., W. Crawford, S. Singh, M. Cannat, V. Combier, and H. Carton (2007), Seismic velocity structure of the upper oceanic crust beneath the Lucky Strike hydrothermal vent field, Mid-Atlantic Ridge, *Geophys. Res. Abstr.*, *9*, A-02386.

Siméoni, P., J. Sarrazin, H. Nouzé, P. M. Sarradin, H. Ondréas, C. Scalabrin, and J. M. Sinquin (2007), Victor 6000: New high-resolution tools for deep sea research, paper presented at Oceans 2007, Mar. Technol. Soc., Vancouver, British Columbia, Canada.

Singh, S. C., W. C. Crawford, H. Carton, T. Seher, V. Combier, M. Cannat, J. P. Canales, D. Dusunur, J. Escartin, and J. M. Miranda (2006), Discovery of a magma chamber and faults beneath a Mid-Atlantic Ridge hydrothermal field, *Nature*, *442*, 1029–1032, doi:10.1038/nature05105.

Tanaka, A., S. Rosat, K. Kisimoto, and T. Urabe (2007), High-resolution bathymetry using Alvin scanning sonar at the Southern East Pacific Rise and its implication to the formation of collapsed lava lakes, *Earth Planets Space*, *59*, 245–249.

Tazieff, H. (1984), Mt Niragongo: Renewed activity of the lava lake, *J. Volcanol. Geotherm. Res.*, *20*, 267–280, doi:10.1016/0377-0273(84)90043-X.

Tilling, R. I. (1987), Fluctuations in surface height of active lava lakes during 1972–1974 Mauna Ulu eruption, Kilauea volcano, Hawaii, *J. Geophys. Res.*, *92*(B13), 13,721–13,730, doi:10.1029/JB092iB13p13721.

Von Damm, K., A. M. Bray, L. G. Buttermore, and S. E. Oosting (1998), The geochemical controls on vent fluids from the Lucky Strike vent field, Mid-Atlantic Ridge, *Earth Planet. Sci. Lett.*, *160*, 521–536, doi:10.1016/S0012-821X(98)00108-3.

Wilson, C., J. L. Charlou, E. Ludford, G. Klinkhammer, C. Chin, H. Bougault, C. German, K. Speer, and M. Palmer (1996), Hydrothermal anomalies in the Lucky Strike segment on the Mid-Atlantic Ridge (37°17′N), *Earth Planet. Sci. Lett.*, *142*, 467–477, doi:10.1016/0012-821X(96)00100-8.

Witham, F., and E. W. Llewellin (2006), Stability of lava lake, *J. Volcanol. Geotherm. Res.*, *158*(3–4), 321–332, doi:10.1016/j.jvolgeores.2006.07.004.